ELSEVIER

Journal of Biomechanics 34 (2001) 1077–1083

JOURNAL OF BIOMECHANICS

www.elsevier.com/locate/jbiomech
www.JBiomech.com

Technical note

Predictive algorithms for neuromuscular control of human locomotion

Matthew L. Kaplan, Jean H. Heegaard*

Division of Biomechanical Engineering, Department of Mechanical Engineering, Stanford University, Durand 259, Stanford, CA 94305-4040, USA

Accepted 18 March 2001

Abstract

The problem of quantifying muscular activity of the human body can be formulated as an optimal control problem. The current methods used with large-scale biomechanical systems are non-derivative techniques. These methods are costly, as they require numerous integrations of the equations of motion. Additionally, the convergence is slow, making them impractical for use with large systems. We apply an efficient numerical algorithm to the biomechanical optimal control problem. Using direct collocation with a trapezoidal discretization, the equations of motion are converted into a set of algebraic constraint equations. An augmented Lagrangian formulation is used for the optimization problem to handle both equality and inequality constraints. The resulting min–max problem is solved with a generalized Newton method. In contrast to the prevalent optimal control implementations, we calculate analytical first- and second-derivative information and obtain local quadratic convergence. To demonstrate the efficacy of the method, we solve a steady-state pedaling problem with 7 segments and 18 independent muscle groups. The computed muscle activations compare well with experimental EMG data. The computational effort is significantly reduced and solution times are a fraction of those of the non-derivative techniques.

Keywords: Optimal control; Steady-state pedaling; Muscle activation; Direct collocation

1. Introduction

Human motion involves a complex coordination of the many muscles of the body. Knowledge of muscular activation patterns can lead to numerous clinical benefits including functional neuromuscular stimulation of paraplegics and rehabilitation. Additionally, to study joint and bone mechanics it is necessary to quantify the boundary loads, generated by muscular activity. Invasive in vivo methods are impractical and electromyography (EMG) data are difficult to quantify. Computer models offer a non-invasive and pliable method of studying muscular control during locomotion.

The human musculoskeletal system is characterized by redundant muscles—more than a single muscle may serve to flex or extend a joint. Due to this redundancy, optimization techniques are used to determine the role of individual muscles. Optimal control techniques have been successfully used to quantify neuromuscular excitations during human motion. The methods currently being used to solve the optimal control problem are computationally expensive. The cost of numerous numerical integrations of the differential equations, together with the slow convergence behavior of these approaches, results in a time-consuming effort, where solution times are typically measured in days or months on current workstations. To investigate muscular action for large biomechanical systems, a more efficient optimal control solution technique is necessary. In this note, we present a computationally fast optimal control solution algorithm. We illustrate the efficacy of the method by solving a steady-state pedaling problem using a 7 segment model with 18 muscles.

2. Problem statement

Finding the neural excitations necessary for steady-state pedaling is described here using an optimal control framework. In optimal control problems, the set of

*Corresponding author. Tel.: +1-650-723-3585; fax: +1-650-723-1778.

E-mail address: heegaard@bonechip.stanford.edu (J. H. Heegaard).

0021-9290/01/$ - see front matter
PII: S0021-9290(01)00057-4

control functions that minimize a given measure of cost is sought. This cost describes the task and is in general a function of the control variables, $\boldsymbol{u}(t)$, and state variables, $\boldsymbol{y}(t)$, at the final time and over the time interval of interest,

$$\min_{\boldsymbol{u}} J \coloneqq \phi(\boldsymbol{y}(t_f)) + \int_0^T L(\boldsymbol{y}, \boldsymbol{u}, t)\,\mathrm{d}t. \tag{1}$$

The state variables and control variables are related by differential equations,

$$\boldsymbol{f}(\boldsymbol{y}, \boldsymbol{u}, t) = \boldsymbol{0}, \tag{2}$$

describing the evolution of the state variables, $\boldsymbol{y}$, in terms of the system's dynamics. Additionally, the musculoskeletal model may be subjected to inequality constraints of the form:

$$\boldsymbol{g}_u(\boldsymbol{u}) \geqslant \boldsymbol{0}, \tag{3}$$

expressing bounds on the neural excitation control variables.

3. Current methods

The problem of human neuromuscular control has been solved for various aspects of gait (e.g., Chow and Jacobson, 1971; Chao and Rim, 1973; Chou et al., 1993), of pedaling (e.g., Levine et al., 1989; Raasch et al., 1997), of kicking (e.g., Hatze, 1976; Audu and Davy, 1988), of jumping (e.g., Anderson et al., 1995; van Soest et al., 1993; Selbie and Caldwell, 1996; Spagele et al., 1999) and of other human motions (Ghosh and Boykin, 1976; Yamaguchi et al., 1995), using a legion of numerical methods. Complex large-scale musculoskeletal optimal control problems are commonly solved with non-derivative methods, such as numerical gradients (e.g., Pandy et al., 1992) and simulated annealing (e.g., Neptune and Hull, 1998). These techniques treat only the control variables as unknown; the state variables are determined by integrating the differential equations of motion using a set of control variables. The control variables are discretized in time into a set of unknowns using nodal values or polynomial interpolations. The cost is then minimized with respect to these parameters using nonlinear programming methods. Assuming a nodal discretization with N discrete nodes in time and m control functions, there are $M = Nm$ optimization parameters, $\boldsymbol{U}$. Analytical derivatives cannot be calculated. Instead, the equations of motion are solved repeatedly at each iteration. The gradient of the cost function with respect to the optimization parameters is calculated numerically based on finite-difference approximations such as forward differences,

$$\frac{\partial J}{\partial U_i} = \frac{1}{h_i}(J(\boldsymbol{U} + h_i\boldsymbol{e}_i) - J(\boldsymbol{U})) + O(h) \quad (i = 1, \ldots, M), \tag{4}$$

where h_i is the ith finite-difference interval and $h_i\boldsymbol{e}_i$ (no sum on i) is a perturbation of the ith component of $\boldsymbol{U}$. These approximate derivative calculations are costly, as the equations of motion must be solved M times for each numerical evaluation of the derivative.

4. Second-order direct collocation

To solve the large-scale biomechanical optimal control problem, we apply a method which is computationally fast and easily amenable to equality and inequality constraints on both state and control variables. We use a direct collocation method to discretize the differential equations. Direct collocation methods together with nonlinear programming have been effectively applied to optimal control problems in the field of trajectory optimization (e.g., Hargraves and Paris, 1987; Enright and Conway, 1991; Betts and Huffman, 1992). We treat the resulting constrained optimization problem with an augmented Lagrangian technique employing analytical first- and second-derivative information, in contrast to prevalent optimal control software. The augmented Lagrangian formulation forms a saddle-point problem, which is solved with a generalized Newton method, resulting in local quadratic convergence.

The state and control variables are both treated as unknown. These variables are discretized in time into a set of nodal values,

$$\boldsymbol{Y} = \{\boldsymbol{y}_a(t)\}_{a=1}^{n_{\text{nodes}}} \quad \text{where } \boldsymbol{y}_a(t) \coloneqq \boldsymbol{y}(t_a), \tag{5}$$

$$\boldsymbol{U} = \{\boldsymbol{u}_d(t)\}_{d=1}^{n_{\text{unodes}}} \quad \text{where } \boldsymbol{u}_d(t) \coloneqq \boldsymbol{u}(t_d). \tag{6}$$

The equations of motion are converted into algebraic constraint equations in the unknown discrete variables using direct collocation with a trapezoidal discretization (Stoer and Bulirsch, 1980). At each temporal node, a, a set of equality constraints, $\boldsymbol{z}_a(\boldsymbol{y}_a, \boldsymbol{y}_{a-1}) = \boldsymbol{0}$, representing the discretized equations of motion, is formed. These equations are assembled over the entire time interval into a collection of the nodal equations,

$$\boldsymbol{Z} = \{\boldsymbol{z}_a\}_{a=1}^{n_{\text{nodes}}} = \boldsymbol{0}. \tag{7}$$

Likewise, the cost function, J, is approximated by a discrete version, J^h, using numerical quadrature:

$$J(\boldsymbol{y}, \boldsymbol{u}) \approx J^h(\boldsymbol{Y}, \boldsymbol{U}), \tag{8}$$

$$J^h(\boldsymbol{Y}, \boldsymbol{U}) = \phi(\boldsymbol{Y}_{n_{\text{nodes}}}) + \frac{\mathrm{d}t}{3}\Bigg[L(\boldsymbol{Y}_1, \boldsymbol{U}_1) + L(\boldsymbol{Y}_{n_{\text{nodes}}}, \boldsymbol{U}_{n_{\text{nodes}}}) + 4\sum_{\substack{a=2 \\ a \text{ even}}}^{n_{\text{nodes}}-1} L(\boldsymbol{Y}_a, \boldsymbol{U}_a) + 2\sum_{\substack{a=3 \\ a \text{ odd}}}^{n_{\text{nodes}}-2} L(\boldsymbol{Y}_a, \boldsymbol{U}_a)\Bigg]. \tag{9}$$

The inequality constraints are discretized at each node by replacing the continuous variables with their discrete counterparts:

$$\boldsymbol{G}_U(\boldsymbol{U}) = \{\boldsymbol{g}(\boldsymbol{u}_d)\}_{d=1}^{n_{\text{unodes}}} \geqslant \boldsymbol{0}. \tag{10}$$

Using the discretizations above, the optimal control problem is converted into a constrained optimization problem,

$$\min_{\boldsymbol{U}} J^h(\boldsymbol{Y}, \boldsymbol{U}), \tag{11}$$

$$\boldsymbol{Z}(\boldsymbol{Y}, \boldsymbol{U}) = \boldsymbol{0}, \tag{12}$$

$$\boldsymbol{G}_U(\boldsymbol{U}) \geqslant \boldsymbol{0}. \tag{13}$$

We reformulate the problem into an unconstrained one using an augmented Lagrangian approach to enforce both the equality and inequality constraints. The optimization problem is transformed into a saddle-point problem where the augmented Lagrangian is minimized with respect to $\boldsymbol{Y}$ and $\boldsymbol{U}$ and maximized with respect to $\boldsymbol{\lambda}_Z$ and $\boldsymbol{\lambda}_U$,

$$\min_{\boldsymbol{Y},\boldsymbol{U}} \max_{\boldsymbol{\lambda}_Z,\boldsymbol{\lambda}_U} \Lambda^r \coloneqq J^h + \boldsymbol{\lambda}_Z \cdot \boldsymbol{Z} + \frac{1}{2} r_z \boldsymbol{Z} \cdot \boldsymbol{Z} - \frac{1}{2r_u} \|\boldsymbol{\lambda}_U\|^2 + \frac{1}{2r_u} \operatorname{dist}^2[\boldsymbol{\lambda}_U^r, \mathbb{R}_+^m], \tag{14}$$

where $\boldsymbol{\lambda}_Z$ is the vector of Lagrange multipliers corresponding to the equality constraints, $\boldsymbol{\lambda}_U$ contains the Lagrange multipliers corresponding to the inequality constraints on the $\boldsymbol{U}$ variables, and r_z and r_u are the regularization parameters corresponding to the equality and inequality constraints, respectively (Alart and Curnier, 1991; Heegaard and Curnier, 1993). The augmented multiplier vector, $\boldsymbol{\lambda}_U^r$, is defined as

$$\boldsymbol{\lambda}_U^r = \boldsymbol{\lambda}_U + r_u \boldsymbol{G}_U, \tag{15}$$

and $\operatorname{dist}^2[\boldsymbol{\lambda}_U^r, \mathbb{R}_+^m]$ is the square of the distance of $\boldsymbol{\lambda}_U^r$ to $\mathbb{R}_+^m$, defined as

$$\operatorname{dist}^2[\boldsymbol{\lambda}_U^r, \mathbb{R}_+^m] = \sum_{i=1}^{m} [\max(0, -\boldsymbol{\lambda}_{Ui}^r)]^2, \tag{16}$$

where m is the total number of nodal control variables. We calculate analytical gradients and Hessians of the augmented Lagrangian with respect to $\boldsymbol{Y}$, $\boldsymbol{U}$, $\boldsymbol{\lambda}_Z$ and $\boldsymbol{\lambda}_U$. The gradient, $\boldsymbol{E}$, defined as

$$\boldsymbol{E}(\boldsymbol{Y}, \boldsymbol{U}, \boldsymbol{\lambda}_Z, \boldsymbol{\lambda}_U) = \begin{Bmatrix} \nabla_{\boldsymbol{Y}} \Lambda^r \\ \nabla_{\boldsymbol{U}} \Lambda^r \\ \nabla_{\boldsymbol{\lambda}_Z} \Lambda^r \\ \nabla_{\boldsymbol{\lambda}_U} \Lambda^r \end{Bmatrix} \tag{17}$$

will be zero at a stationary point, $\{\boldsymbol{Y}^*, \boldsymbol{U}^*, \boldsymbol{\lambda}_Z^*, \boldsymbol{\lambda}_U^*\}$, i.e.,

$$\boldsymbol{E}(\boldsymbol{Y}^*, \boldsymbol{U}^*, \boldsymbol{\lambda}_Z^*, \boldsymbol{\lambda}_U^*) = \boldsymbol{0}. \tag{18}$$

The Hessian is formed by taking the derivative of the gradient $\boldsymbol{E}$:

$$\nabla \boldsymbol{E} = \nabla^2 \Lambda^r = \begin{bmatrix} \nabla^2_{\boldsymbol{YY}} \Lambda^r & \nabla_{\boldsymbol{U}} \nabla_{\boldsymbol{Y}} \Lambda^r & \nabla_{\boldsymbol{\lambda}_Z} \nabla_{\boldsymbol{Y}} \Lambda^r & \nabla_{\boldsymbol{\lambda}_U} \nabla_{\boldsymbol{Y}} \Lambda^r \\ \nabla_{\boldsymbol{Y}} \nabla_{\boldsymbol{U}} \Lambda^r & \nabla^2_{\boldsymbol{UU}} \Lambda^r & \nabla_{\boldsymbol{\lambda}_Z} \nabla_{\boldsymbol{U}} \Lambda^r & \nabla_{\boldsymbol{\lambda}_U} \nabla_{\boldsymbol{U}} \Lambda^r \\ \nabla_{\boldsymbol{Y}} \nabla_{\boldsymbol{\lambda}_Z} \Lambda^r & \nabla_{\boldsymbol{U}} \nabla_{\boldsymbol{\lambda}_Z} \Lambda^r & \nabla^2_{\boldsymbol{\lambda}_Z \boldsymbol{\lambda}_Z} \Lambda^r & \nabla_{\boldsymbol{\lambda}_U} \nabla_{\boldsymbol{\lambda}_Z} \Lambda^r \\ \nabla_{\boldsymbol{Y}} \nabla_{\boldsymbol{\lambda}_U} \Lambda^r & \nabla_{\boldsymbol{U}} \nabla_{\boldsymbol{\lambda}_U} \Lambda^r & \nabla_{\boldsymbol{\lambda}_Z} \nabla_{\boldsymbol{\lambda}_U} \Lambda^r & \nabla^2_{\boldsymbol{\lambda}_U \boldsymbol{\lambda}_U} \Lambda^r \end{bmatrix}. \tag{19}$$

The Hessian is extremely sparse and well-suited for efficient solutions to the linear problem. We use a direct banded solver together with a reverse Cuthill–McKee bandwidth reduction reordering scheme (George, 1971) to improve the speed of the matrix solution procedure. Due to the sparsity, the matrix solution time scales well as the size of the system increases.

To solve the saddle-point problem, we update the primal variables, $\boldsymbol{Y}$ and $\boldsymbol{U}$, and dual variables, $\boldsymbol{\lambda}_Z$ and $\boldsymbol{\lambda}_U$, simultaneously at each iteration, k, using the Newton Raphson method,

$$\boldsymbol{X}^{(k+1)} = \boldsymbol{X}^{(k)} + \alpha^{(k)} \boldsymbol{d}^{(k)}, \tag{20}$$

where $\boldsymbol{X}$ is the vector of all unknowns,

$$\boldsymbol{X} = \{\boldsymbol{Y}, \boldsymbol{U}, \boldsymbol{\lambda}_Z, \boldsymbol{\lambda}_U\}. \tag{21}$$

The Newton search direction, $\boldsymbol{d}^{(k)}$, at the kth iteration is defined as

$$\boldsymbol{d}^{(k)} = -[\nabla^2_{\boldsymbol{X}} \Lambda^r(\boldsymbol{X})^{(k)}]^{-1} \nabla_{\boldsymbol{X}} \Lambda^r(\boldsymbol{X})^{(k)}, \tag{22}$$

and is scaled by a line search factor α, defined by

$$\min_{\alpha} \phi(\boldsymbol{X}^{(k)} + \alpha \boldsymbol{d}^{(k)}), \tag{23}$$

where ϕ is the scalar function

$$\phi(\boldsymbol{X}) = \tfrac{1}{2} \nabla_{\boldsymbol{X}} \Lambda^r(\boldsymbol{X}) \cdot \nabla_{\boldsymbol{X}} \Lambda^r(\boldsymbol{X}). \tag{24}$$

5. Simplified pedaling problem

In order to compare the numerical efficiency of the second-order collocation method with a numerical gradient method, we solve a simplified steady-state pedaling problem with a single control function in the form of a net crank torque (see Fig. 1). The cost function expresses the variation in angular velocity of the crank from the initial angular velocity:

$$J = \int_0^{t_f} (\dot{q}_1(t) - \dot{q}_1(0))^2 \, \mathrm{d}t, \tag{25}$$

where $\dot{q}_1(t)$ is the crank angular velocity. Both approaches are able to accomplish well the goal of maintaining a constant crank angular velocity. The numerical gradient approach involves many fewer unknowns, but is hindered by slow convergence and

costly iterations. The direct collocation method, although employing many more unknowns, converges more quickly and in fewer iterations. The scaling of solution times as the size of the system increases is significantly more favorable for the direct collocation method, indicating that this method is better suited to solving large-scale optimal control problems. Fig. 2 illustrates the total solution time scaling as the number of nodes increases for the simple pedaling problem. The difference in computational cost of the two methods grows as the size of the system increases; the ratio of solution times is 6 for the case of 21 nodes and 240 for 301 nodes.

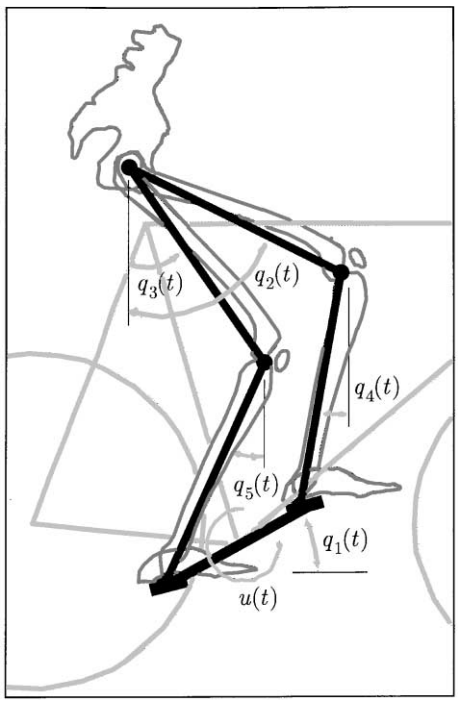

Fig. 1. Simplified pedaling model.

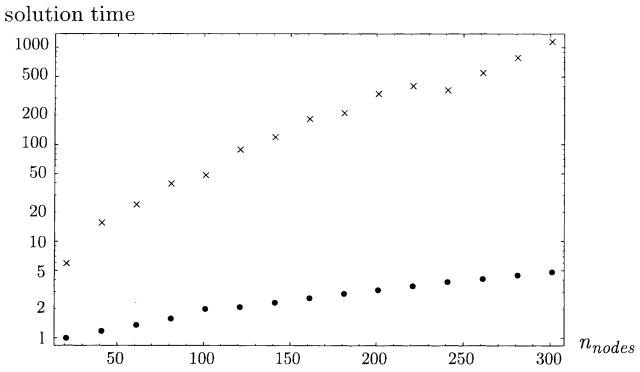

Fig. 2. Normalized solution times on a log scale from the numerical gradient (×) and direct collocation (●) methods for the simple pedaling problem versus the number of nodes. The normalized solution cost for the collocation method ranges between 1 and 5, while for the same problems the solution time for the numerical gradient method runs between 6 and 1200.

6. Pedaling problem

The effectiveness of our control algorithm to predict muscle activation during human locomotion was tested by simulating a pedaling experiment. Pedaling was chosen as a convenient model of human motion as it avoids the effects of postural instability present in gait and offers a simple way to vary loading, cadence and limb phasing (Ting et al., 1999).

We solve a large-scale two-dimensional pedaling problem with 7 segments and 18 muscles to determine the muscle activation patterns for the coordination of steady-state pedaling. Fig. 3 illustrates the nine muscle groups per leg and the dynamical model with seven generalized coordinates. The origin and insertion sites of the muscles are based on the data of Delp et al. (1990), with added geometric assumptions. The model is two dimensional and, except for the rectus femoris and vasti, the muscles are taken to act along straight lines.

The muscles are modeled using a Hill muscle model with force–velocity and force–length dependence (Zajac, 1989). The total muscle force, F^M, is the sum of an active force, F^{CE}, produced in the Hill contractile element, and a passive contribution, F^{PE},

$$F^M[a(t), l^M(t), v^M(t)] = F^{PE}[l^M(t)] + F^{CE}[a(t), l^M(t), v^M(t)], \quad (26)$$

where $a(t)$ is the muscle activation, $l^M(t)$ is the current length of the muscle, and $v^M(t)$ is the rate of shortening. The excitation–contraction dynamics relating the neural signals to the muscle activations is represented by nonlinear first-order differential equations (Raasch et al., 1997),

$$\dot{a}(t) = \begin{cases} (u(t) - a(t))(c_1 u(t) + c_2) & u(t) \geqslant a(t), \\ (u(t) - a(t))c_2 & u(t) < a(t), \end{cases} \quad (27)$$

where

$$c_1 = \frac{1}{\tau_{\text{rise}}} - \frac{1}{\tau_{\text{fall}}}, \quad (28)$$

$$c_2 = \frac{1}{\tau_{\text{fall}}}, \quad (29)$$

and where $u(t)$ is the neural signal, and τ_{rise} and τ_{fall} are the rise and fall time constants.

We solve the optimal control problem to find the neural excitation signals that produce steady-state motion at 60 rpm against a workload of 120 J/cycle. The cost function is chosen so that at the converged solution the angular velocity of the crank is 60 rpm and the pedal angles over the crank cycle

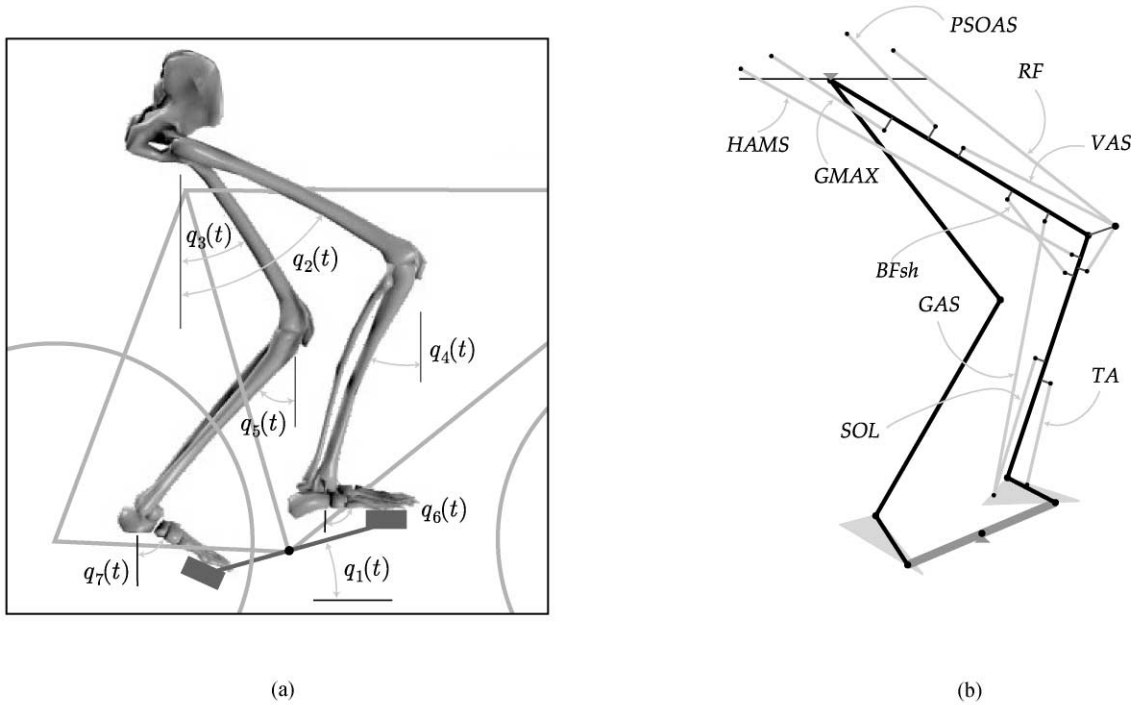

(a) (b)

Fig. 3. (a) Pedaling model dynamics. Shown are the generalized coordinates, $\boldsymbol{q}$. (b) Pedaling model muscles. The muscles are shown for a single leg only. The labeling corresponds to the following muscle groups: psoas (PSOAS), rectus femoris (RF), vasti (VAS), gluteus maximus (GMAX), hamstrings (HAMS), biceps femoris short (BFsh), gastrocnemius (GAS), soleus (SOL) and tibialis anterior (TA).

match experimental pedal angle data from Ting et al. (1999):

$$J = \int_0^{t_f} \left[w_1(s_1(t) - s_1(0))^2 + w_2((q_6(t) - q_6^p(\theta(t)))^2 + (q_7(t) - q_7^p(\theta(t)))^2) + w_3 \sum_0^{n_{cf}} u_i^2 \right] \mathrm{d}t, \tag{30}$$

where $s_1(t)$ is the quasi-velocity corresponding to the crank angular velocity, $q_6(t)$ and $q_7(t)$ are the feet angles, $q_6^p(t)$ and $q_7^p(t)$ are the feet angles corresponding to the experimental pedal data, and $w_1 - w_3$ are weights given to the different components of the cost function. We solve the problem for two cycles to ignore any spurious behavior at the start time. Using a time step of 0.01 s, the problem involves 30,000 unknown variables. The optimal control simulation produces kinematics consistent with the desired motion specified by the cost function. We compare the muscle activation results with experimental EMG measurements from Ting et al. (1999) (see Fig. 4). Good qualitative agreement between the calculated muscle activations and experimental averaged EMG data is obtained. Both the phasing and the magnitudes of the muscle activations match well with the experimental results for the five coincident muscles from the experiment and the simulation.

7. Discussion

We have presented a new algorithm based on optimal control to solve the problem of finding the neural excitation signals necessary for coordination of human movement. Existing approaches to solve complex biomechanical optimal control problems have typically implemented numerical gradient or simulated annealing methods. These algorithms, although capable of producing converged solutions, require lengthy computation times. In contrast to these methods, the algorithm described here introduces an optimal control solution technique with the ability to solve large-scale biomechanical systems in a dramatically decreased time. This approach, using direct collocation and nonlinear programming, differs fundamentally from the prevalent methods adopted for neuromuscular control studies of human locomotion. In most current techniques, the control functions are treated as unknown and the state variables are calculated from a given set of controls using an explicit forward integration of the differential equations of motion. The algorithm performance is degraded by the expense of numerous forward integrations and by linear convergence. We assume a significantly larger group of variables, considering both the state and control variables as unknown. All quantities are discretized in time and the resulting nonlinear programming problem is solved a single

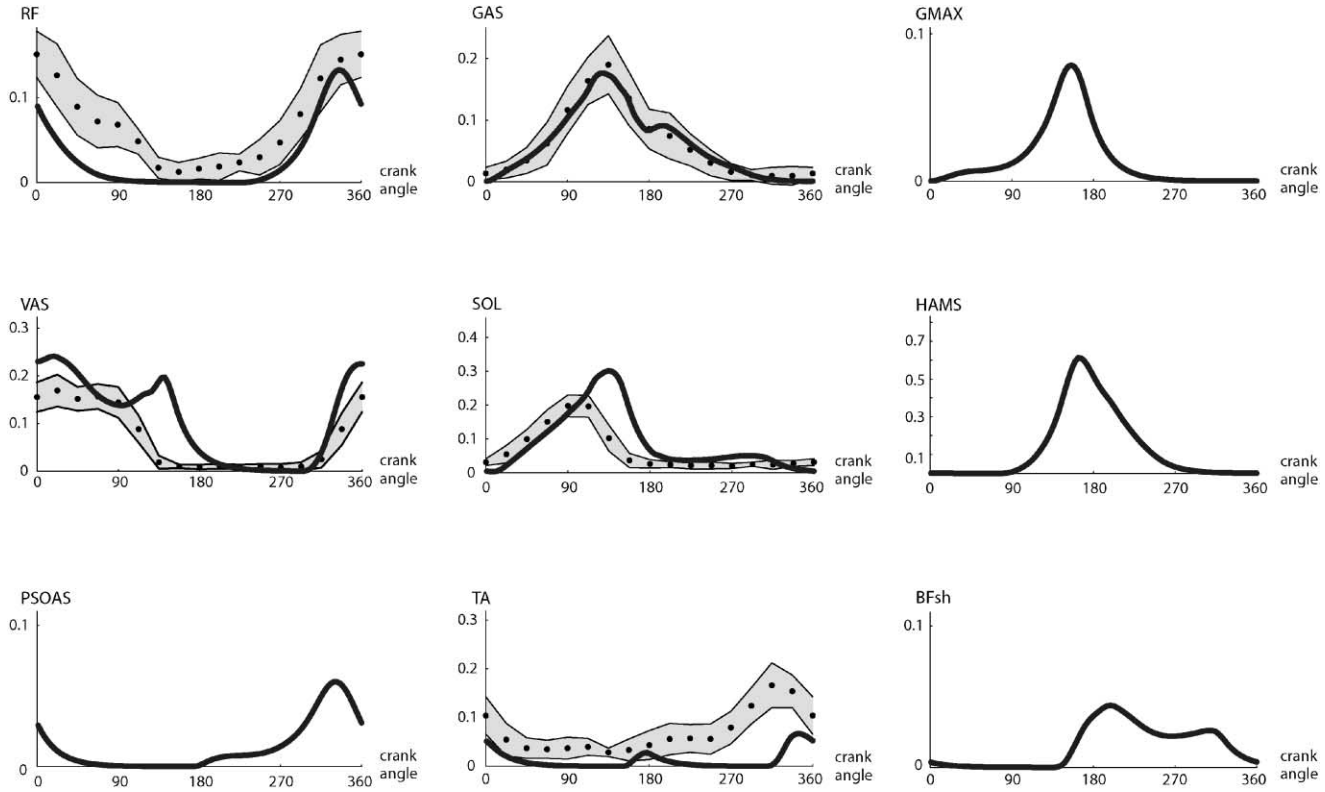

Fig. 4. Normalized EMG data for the five muscles, RF (rectus femoris), VAS (vasti), GAS (gastrocnemius), SOL (soleus) and TA (tibialis anterior), together with calculated muscle activations for these muscles and for PSOAS (psoas), GMAX (gluteus maximus), HAMS (hamstrings) and BFsh (biceps femoris short). The points are the averaged EMG values and the shaded areas represent one standard deviation. The solid lines are the predicted muscle activations.

time. In this way, the cost associated with the multiple solutions to the equations of motion is eliminated. Moreover, we analytically form first and second derivatives and are able to use second-order minimization techniques with local quadratic convergence properties.

We compared the solution times for a simplified pedaling problem using the second-order direct collocation method and a numerical gradient method. The computational effort was significantly less using the direct collocation approach. This difference increased as the size of the system grew, indicating that the second-order algorithm is better suited to solving large-scale neuromuscular control problems.

Using the proposed method, the solution time for the steady-state pedaling problem was significantly shorter than those using other optimal control algorithms. We considered a musculoskeletal model with 18 independent muscles, each represented by a Hill-type muscle model with force–length dependence, force–velocity dependence and activation dynamics. Ting (2000) used a numerical gradient approach on a pedaling problem with 9 muscles and 27 unknowns, representing a signal onset time, a magnitude and a duration. The solution took on the order of a week to converge. Neptune (2000) solved a pedaling problem, also with 9 muscles and 27 unknowns, using simulated annealing in 3–4 days. Using a second-order method, convergence times for our pedaling model ranged from 20 min to 3 h, for the cases requiring continuation steps to ensure global convergence. The computer architectures in all cases were similar modern workstations (e.g., single processor SGI Octane).

The predicted activation histories compared well with experimental EMG data, illustrating the possibility of using this method for coordination studies on systems with great complexity. This technique is well suited for solving biomechanical optimal control problems with physiologically accurate geometry, joints and muscles. Possibilities for future studies include the simulation of whole-body locomotion tasks under healthy and pathological conditions.

Acknowledgements

This work was supported in part by grants from the Whitaker Foundation and the Powell Foundation.

References

Alart, P., Curnier, A., 1991. A mixed formulation for frictional contact problems prone to Newton like methods. Comparitive Methods in Applied Mechanics and Engineering 92, 353–375.

Anderson, F.C., Ziegler, J.M., Pandy, M.G., Whalen, R.T., 1995. Application of high-performance computing to numerical simulation of human movement. Journal of Biomechanics and Engineering 117, 155–157.

Audu, M.L., Davy, D.T., 1988. A comparison of optimal control algorithms for complex bioengineering studies. Optimal Control Applications and Methods 9, 101–106.

Betts, J.T., Huffman, W.P., 1992. Application of sparse nonlinear programming to trajectory optimization. Journal of Guidance Control and Dynamics 15, 198–206.

Chao, E.Y., Rim, K., 1973. Application of optimization principles in determining the applied moments in human leg joints during gait. Journal of Biomechanics 6, 497–510.

Chou, L.S., Draganich, L.F., Song, S.M., 1993. Predicting the kinematics and kinetics of gait using dynamic programming. Advances in Bioengineering BED, Vol. 26, ASME, New York, pp. 523–526.

Chow, C.K., Jacobson, D.H., 1971. Studies of human locomotion via optimal programming. Mathematical Biosciences 10, 239–306.

Delp, S.L., Loan, P., Hoy, M.G., Zajac, F.E., Topp, E.L., Rosen, J.M., 1990. An interactive graphics-based model of the lower extremity to study orthopaedic surgical procedures. IEEE Transactions on Biomedical Engineering 37, 757–767.

Enright, P.J., Conway, B.A., 1991. Optimal finite-thrust spacecraft trajectories using collocation and nonlinear programming. Journal of Guidance Control and Dynamics 14, 981–985.

George, A., 1971. Computer implementation of the finite element method. Ph.D. Thesis, Stanford University.

Ghosh, T.K., Boykin, J., 1976. Analytic determination of an optimal human motion. Journal of Optimization Theory and Applications 19, 327–346.

Hargraves, C.R., Paris, S.W., 1987. Direct trajectory optimization using nonlinear programming and collocation. Journal of Guidance Control and Dynamics 10, 338–342.

Hatze, H., 1976. The complete optimization of a human motion. Mathematical Biosciences 28, 99–135.

Heegaard, J.H., Curnier, A., 1993. An augmented Lagrangian method for discrete large-slip contact problems. International Journal of Numerical Methods in Engineering 36, 569–593.

Levine, W.S., Ma, B., Zajac, F.E., 1989. The dynamics and optimal controls for some simplified models of pedaling a stationary bicycle. Proceedings of the 23rd Annual Conference on Information Sciences and Systems, pp. 567–573.

Neptune, R.R., 2000. Personal communication.

Neptune, R.R., Hull, M.L., 1998. Evaluation of performance criteria for simulation of submaximal steady-state cycling using a forward dynamic model. Journal of Biomechanical Engineering 120, 334–340.

Pandy, M.G., Anderson, F.C., Hull, D.G., 1992. A parameter optimization approach for the optimal control of large-scale musculoskeletal systems. Journal of Biomechanical Engineering 114, 450–460.

Raasch, C.C., Zajac, F.E., Ma, B., Levine, W.S., 1997. Muscle coordination of maximum-speed pedaling. Journal of Biomechanics 30, 595–602.

Selbie, W.S., Caldwell, G.E., 1996. A simulation study of vertical jumping from different starting postures. Journal of Biomechanics 29, 1137–1146.

Spagele, T., Kistner, A., Gollhofer, A., 1999. Modelling, simulation and optimisation of a human vertical jump. Journal of Biomechanics 32, 521–530.

Stoer, J., Bulirsch, ., 1980. Introduction to Numerical Analysis. Springer, New York.

Ting, L.H., 2000. Personal communication.

Ting, L.H., Kautz, S.A., Brown, D.A., Zajac, F.E., 1999. Phase reversal of biomechanical functions and muscle activity in backward pedaling. Journal of Neurophysics 81, 544–551.

van Soest, A.J., Schwab, A.L., Bobbert, M.F., van Ingen Schenau, G.J., 1993. The influence of the biarticularity of the gastrocnemius on vertical-jumping achievement. Journal of Biomechanics 26, 1–8.

Yamaguchi, G.T., Moran, D.W., Si, J., 1995. A computationally efficient method for solving the redundant problem in biomechanics. Journal of Biomechanics 28, 999–1005.

Zajac, F.E., 1989. Muscle and tendon: properties, models, scaling, and application to biomechanics and motor control. In: Bourne, J.R. (Ed.),, CRC Critical Reviews in Biomedical Engineering, Vol. 17. CRC Press, Boca Raton, Florida, pp. 359–411.